THE JOURNAL OF BIOLOGICAL CHEMISTRY
Vol. 278, No. 47, Issue of November 21, pp. 46307–46320, 2003
Printed in U.S.A.

Differential Voltage-dependent K^+ Channel Responses during Proliferation and Activation in Macrophages*

Received for publication, April 28, 2003, and in revised form, July 31, 2003
Published, JBC Papers in Press, August 15, 2003, DOI 10.1074/jbc.M304388200

Rubén Vicente,[a,b,c] Artur Escalada,[b,d,e] Mireia Coma,[a] Gemma Fuster,[a] Ester Sánchez-Tilló,[f] Carmen López-Iglesias,[g] Concepció Soler,[h,i] Carles Solsona,[d,j] Antonio Celada,[f,k] and Antonio Felipe[a,l]

From the [a]Molecular Physiology Laboratory, Departament de Bioquímica i Biologia Molecular, [g]Unitat de Reconeixement Molecular in Situ, Serveis Cientificotčcnics, [f]Macrophage Biology Group, Biomedical Research Institute of Barcelona, [h]Departament de Fisiologia, Universitat de Barcelona, E-08028 Barcelona, Spain and the [d]Cellular and Molecular Neurobiology Laboratory, Departament de Biologia Cellular i Anatomia Patològica, Universitat de Barcelona-Campus de Bellvitge, E-08907 Hospitalet de Llobregat, Spain

Voltage-dependent K^+ channels (VDPC) are expressed in most mammalian cells and involved in the proliferation and activation of lymphocytes. However, the role of VDPC in macrophage responses is not well established. This study was undertaken to characterize VDPC in macrophages and determine their physiological role during proliferation and activation. Macrophages proliferate until an endotoxic shock halts cell growth and they become activated. By inducing a schedule that is similar to the physiological pattern, we have identified the VDPC in non-transformed bone marrow-derived macrophages and studied their regulation. Patch clamp studies demonstrated that cells expressed outward delayed and inwardly rectifying K^+ currents. Pharmacological data, mRNA, and protein analysis suggest that these currents were mainly mediated by Kv1.3 and Kir2.1 channels. Macrophage colony-stimulating factor-dependent proliferation induced both channels. Lipopolysaccharide (LPS)-induced activation differentially regulated VDPC expression. While Kv1.3 was further induced, Kir2.1 was down-regulated. TNF-α mimicked LPS effects, and studies with TNF-α receptor I/II double knockout mice demonstrated that LPS regulation mediates such expression by TNF-α-dependent and -independent mechanisms. This modulation was dependent on mRNA and protein synthesis. In addition, bone marrow-derived macrophages expressed Kv1.5 mRNA with no apparent regulation. VDPC activities seem to play a critical role during proliferation and activation because not only cell growth, but also inducible nitric-oxide synthase expression were inhibited by blocking their activities. Taken together, our results demonstrate that the differential regulation of VDPC is crucial in intracellular signals determining the specific macrophage response.

Immune system responses to an antigen involve a complex network of several cell types. Among them, the mononuclear phagocyte family comprises numerous cell types, including tissue macrophages, Kupffer cells, dermal Langerhans cells, osteoclasts, microglia, and perhaps some of the interdigitating and follicular dendritic cells from lymphoid organs (1). Macrophages perform critical functions in the immune system, acting as regulators of homeostasis and as effector cells in infection, wounding, and tumor growth. In response to different growth factors and cytokines, macrophages can proliferate, become activated or differentiate. As monocytes differentiate into mature, non-proliferating macrophages they can produce a large variety of responses, including chemotaxis, phagocytosis, and secretion of numerous cytokines and other substances. To elicit the appropriate physiological response plasma membrane protein expression changes dramatically from proliferation to activation (2).

Voltage-dependent potassium channels (VDPC)[1] are a group of plasma membrane ion channels with a key role in controlling repolarization and resting membrane potential in electrically excitable cells. K^+ channels are also involved in the maintenance of vascular smooth muscle tone, glucose-stimulated insulin release by β-pancreatic cells, cell volume regulation, and cell growth (3). Leukocytes express a number of voltage-gated and/or second messenger-modulated ion channels, and the electrophysiological properties of many of these channels are known (4–17). Despite considerable progress, important questions remain unsolved, the relationship of these proteins to cell function being one of the most relevant (18–20). VDPC are associated with macrophage functions such as migration, proliferation, activation, and cytokine production (see Refs. 18 and 19 for reviews). Although microglia appears to express most neuronal channels, circulating macrophages have a number of VDPC yet to be defined (19). These proteins have been studied

* The costs of publication of this article were defrayed in part by the payment of page charges. This article must therefore be hereby marked "*advertisement*" in accordance with 18 U.S.C. Section 1734 solely to indicate this fact.
[b] Both authors contributed equally to this work.
[c] Supported by a fellowship from the Universitat de Barcelona.
[e] Supported by a fellowship from the Fundació Marató TV3.
[i] Supported by Fondo de Investigaciones Sanitarias Grant PI021192 and the "Ramón y Cajal" program from Ministerio de Ciencia y Tecnología (MCYT), Spain.
[j] Supported by The Fundació August Pi i Sunyer, Generalitat de Catalunya and MCYT Grant BFI2001-3331.
[k] Supported by MCYT Grant BMC2001-3040. To whom correspondence may be addressed: Macrophage Biology Group, Biomedical Research Institute of Barcelona, Barcelona Science Park, University of Barcelona, Josep Samitier 1–5, Barcelona E-08028, Spain. Tel.: 34-934037165; Fax: 34-934034747; E-mail: acelada@ub.edu.
[l] Supported by the Universitat de Barcelona and MCYT Grant BFI2002-00764. To whom correspondence may be addressed: Molecular Physiology Laboratory, Departament de Bioquímica i Biologia Molecular, Universitat de Barcelona, Avda. Diagonal 645, E-08028 Barcelona, Spain. Tel.: 34-93-4034616; Fax: 34-93-4021559; E-mail: afelipe@ub.edu.

[1] The abbreviations used are: VDPC, voltage-dependent potassium channels; BMDM, bone marrow-derived macrophages; iNOS, inducible nitric-oxide synthase; LPS, lipopolysaccharide; M-CSF, macrophage-colony stimulating factor; MgTx, rMargatoxin; TNF-α, tumor necrosis factor α; IL, interleukin; RT, reverse transcriptase; PBS, phosphate-buffered saline; ANOVA, analysis of variance.

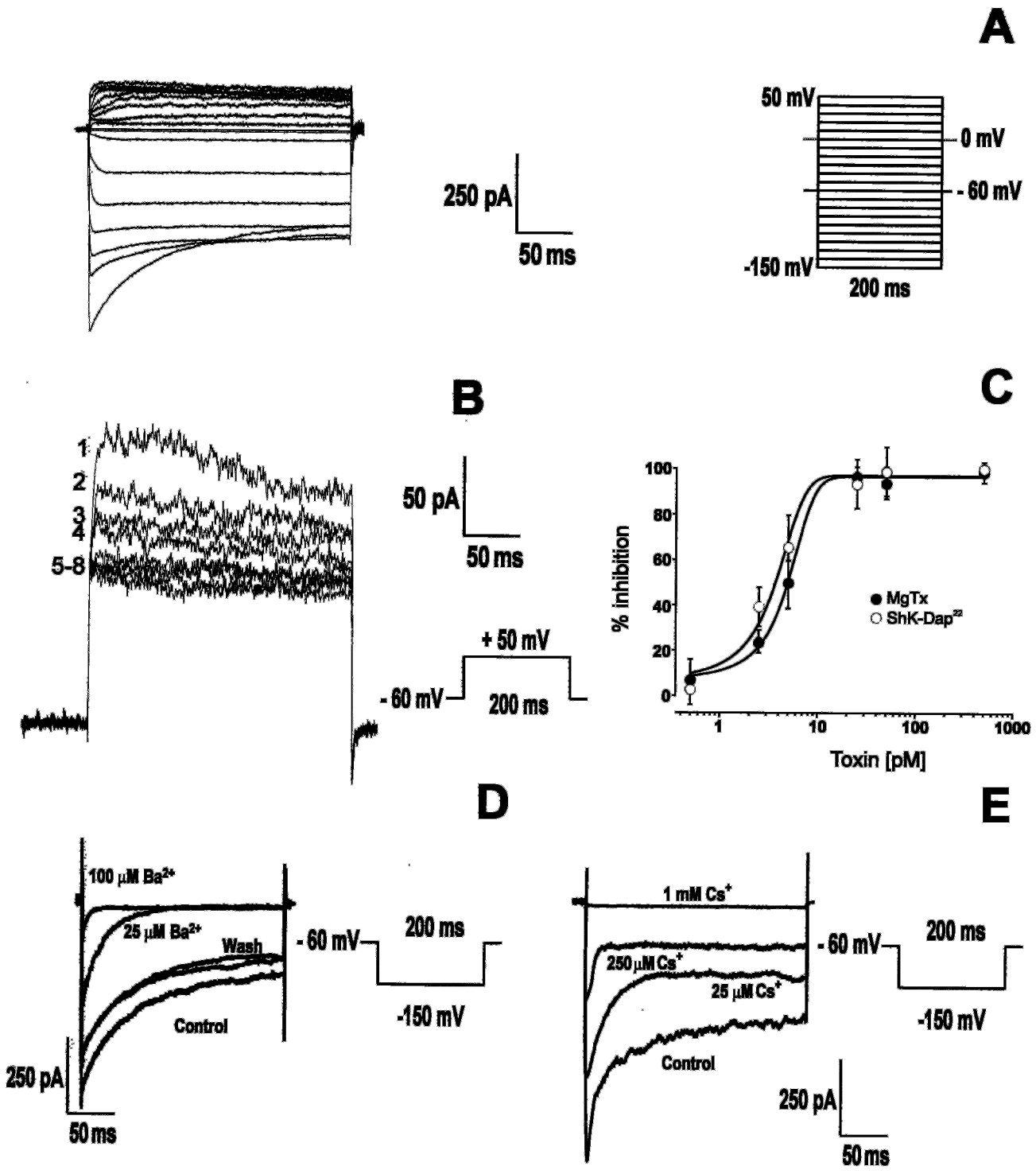

FIG. 1. **Macrophages express outward delayed and inwardly rectifying K^+ currents.** *A*, representative traces of K^+ currents. Cells were held at −60 mV and pulse potentials were applied as indicated. *B*, cumulative inactivation of outward currents. Currents were elicited by a train of 8 depolarizing voltage steps (200 ms duration) to +50 mV once every 400 ms. The current amplitude became progressively smaller from the first trace to the last. *C*, dose-dependent inhibition curves of the outward current by MgTx (●) and ShK-Dap^{22} (○). Currents were evoked at +50 mV from a holding potential of −60 mV during a pulse potential of 200 ms. The percent of inhibition was calculated by comparing the current at a given concentration of toxin *versus* that obtained in its absence. *D*, dose-dependent inhibition of the inwardly rectifying current by Ba^{2+}. *E*, dose-dependent inhibition of the inwardly rectifying current by Cs^+.

in various cellular models, and outward delayed and inwardly rectifying K^+ currents have been identified. Furthermore, the presence of the *shaker*-like Kv1.3 and Kir2.1 channels has been detected in some studies. However, the use of either activated or transformed macrophage cell lines has led to controversial results (4–20). Thus, while a high-conductance Ca^{2+}-dependent K^+ channel has been clearly identified as an early step in transmembrane signal transduction in macrophages (21), the physiological role of VDPC in either proliferation or activation is not known. Primary culture of bone marrow-derived macrophages (BMDM) is a unique non-transformed model in which proliferation and activation can be studied separately, mimick-

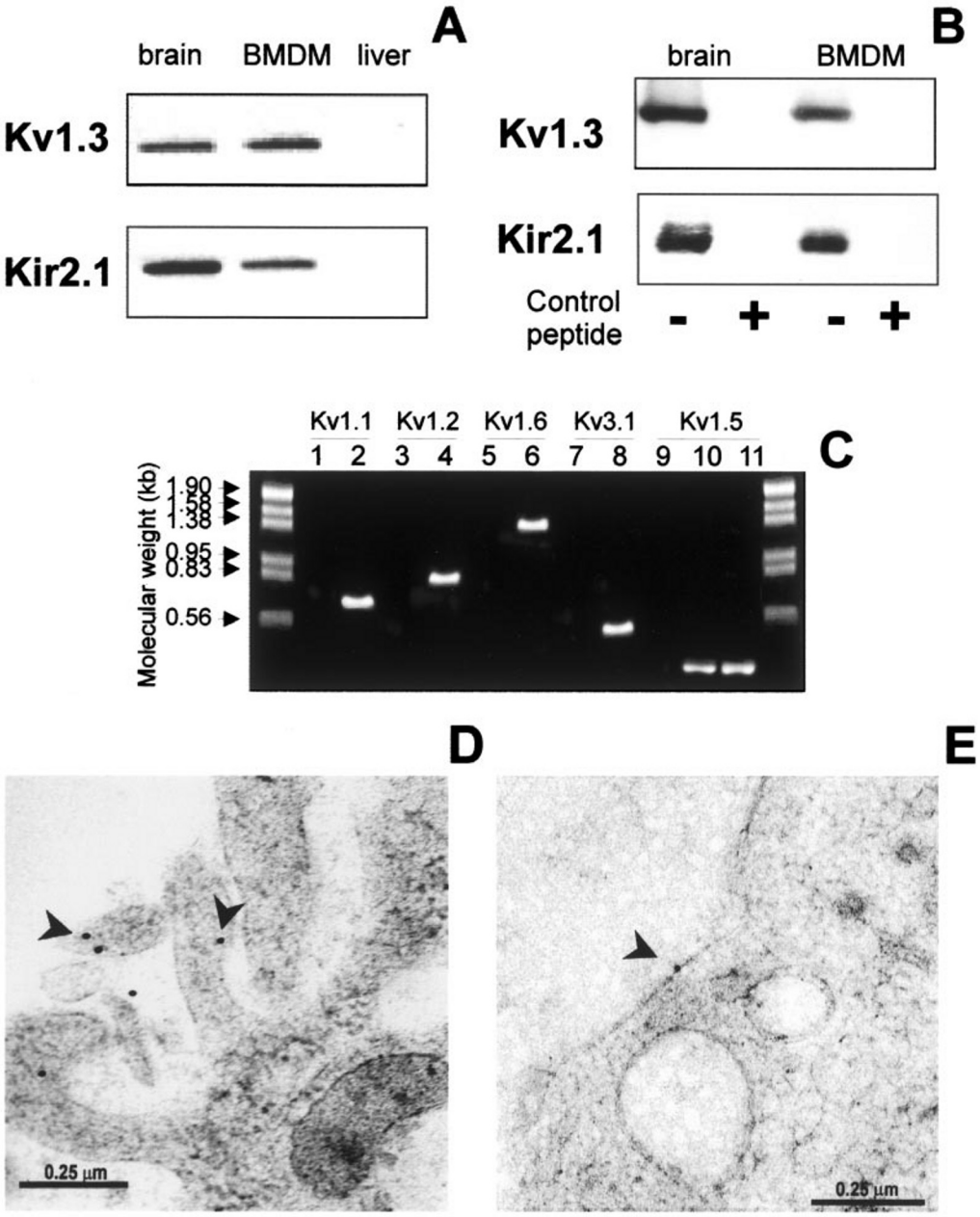

FIG. 2. **Voltage-dependent K^+ channel expression in macrophages.** *A*, mRNA expression of Kv1.3 and Kir2.1 in the mouse brain and macrophages but not in the liver. 1 μg of total RNA was used in RT-PCR reactions as described under "Experimental Procedures." *B*, Kv1.3 and Kir2.1 protein expression in the mouse brain and BMDM. Western blot analysis were performed in the presence and the absence of the control antigen peptide. *C*, VDPC expression in BMDM. RT-PCR was set as described under "Experimental Procedures" with oligonucleotides from Kv1.1 (accession number NM_010595; base pairs 1102–1807), Kv1.2 (accession number NM_008417, base pairs 841–1691), Kv1.5 (accession number AF302768, base pairs 3003–3337), Kv1.6 (accession number NM_013568, base pairs 233–1822), and Kv3.1 (accession number Y07521, base pairs 727–1231). *Lanes 1*, *3*, *5*, *7*, *9*, and *10*, PCR reactions from BMDM. *Lanes 2*, *4*, *6*, *8*, *11*, PCR from mouse brain. *Lane 9* of Kv1.5 is a negative control in the absence of the RT reaction. PCR products were run in a 1% agarose gel. *D* and *E*, immunocytochemical electron microscopic detection of Kv1.3 and Kir2.1 proteins, respectively. *Arrows* show specific channel protein localization. *Bars* indicate 0.25-μm scale.

ing physiological processes that occur in the body (22). Macrophages are generated in the bone marrow and, through the bloodstream, reach all tissues, stop proliferation, and become activated (2). Macrophage colony-stimulating factor (M-CSF) is the specific growth factor for this cell type (23). On the other hand, lipopolysaccharide (LPS) is a major component of the outer Gram-negative bacteria membrane, which interacts with monocytes/macrophages and induces a variety of intracellular signaling cascades, finally leading to the release of endogenous mediators such as TNF-α, IL-1, and IL-6 (24). Furthermore, LPS triggers cellular activation and apoptosis by an early TNF-α-dependent mechanism (25).

Several VDPC candidates could be present in macrophages and our first interest was to identify these channels in a primary culture of BMDM. Macrophages mainly expressed the outward delayed Kv1.3 and the inwardly rectifying Kir2.1 potassium channels. Because VDPC could be involved not only in proliferation but also in activation, our second goal was to determine their specific role by inducing a schedule that is similar to the physiological pattern in BMDM. M-CSF-dependent proliferation led to an up-regulation of VDPC generating an increase in potassium current densities without changes in current kinetics. When cells were further incubated with LPS the electrophysiological properties changed dramatically.

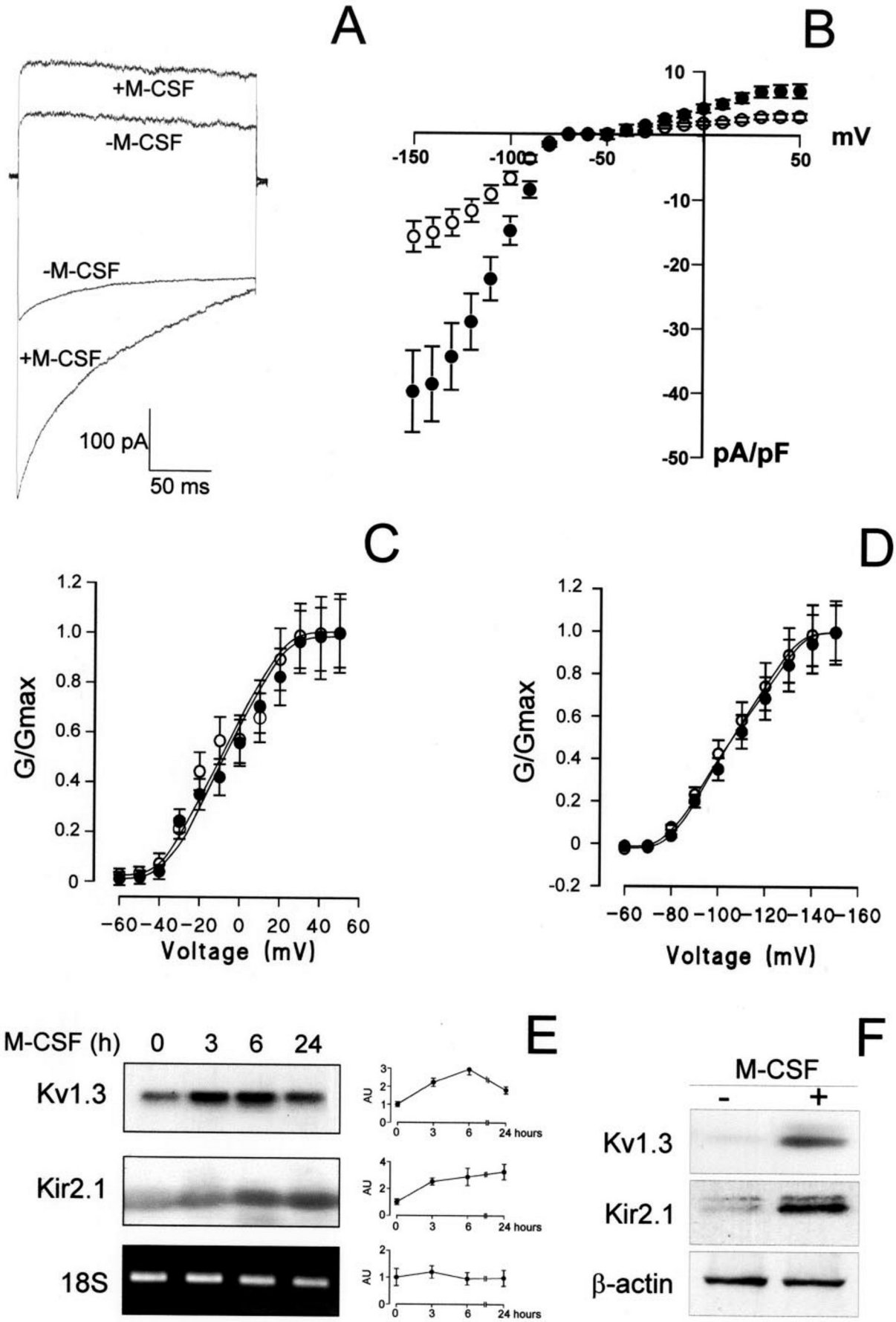

FIG. 3. **M-CSF-dependent proliferation induces VDPC in macrophages.** *A*, cells were incubated for 24 h in the presence (+*M-CSF*) or absence (−*M-CSF*) of the growth factor. Representative outward and inward traces were elicited by a hyperpolarizing step from −60 to −150 mV and a depolarizing step from −60 to +50 mV for 200 ms, respectively. *B*, current density *versus* voltage relationship of K^+ currents. Macrophages

Thus, Kv1.3 was further increased, whereas Kir2.1 was down-regulated. We also show that TNF-α partially mimicked the response to LPS, suggesting that there are TNF-α-dependent and -independent mechanisms mediating LPS-induced VDPC modulation in macrophages. Our results have physiological relevance and indicate that VDPC expression is important as an early regulatory step, and fine-tuning modulation of their expression is crucial to the specific membrane signaling that triggers the appropriate immune response.

EXPERIMENTAL PROCEDURES

Animals and Cell Culture—BMDM from 6- to 10-week-old BALB/c or C57/BL6 mice (Charles River Laboratories) were used. Cells were isolated and cultured as described elsewhere (22). Briefly, animals were killed by cervical dislocation, and both femurs were dissected removing adherent tissue. The ends of bones were cut off and the marrow tissue was flushed by irrigation with medium. The marrow plugs were passed through a 25-gauge needle for dispersion. The cells were cultured in plastic dishes (150 mm) in Dulbecco's modified Eagle's medium containing 20% fetal bovine serum and 30% supernatant of L-929 fibroblast (L-cell) conditioned media as a source of M-CSF. Macrophages were obtained as a homogeneous population of adherent cells after 7 days of culture and maintained at 37 °C in a humidified 5% CO_2 atmosphere. For experiments, they were cultured with the same tissue culture differentiation medium (Dulbecco's modified Eagle's medium, 20% fetal bovine serum, 30% L-cell medium) or arrested at G_0 by M-CSF deprivation in Dulbecco's modified Eagle's medium supplemented with 10% fetal bovine serum for at least 18 h. G_0-arrested cells were further incubated in the absence or presence of recombinant murine M-CSF (1200 units/ml), with or without LPS (100 ng/ml) or TNF-α (100 ng/ml), for the indicated times. In some experiments, cells were exposed to rMargatoxin (MgTx), $BaCl_2$, cycloheximide, and actinomycin D as previously described (26–30).

The TNF-α receptor I/II double knockout mice (C57/BL6) used in this study were generated and characterized as previously reported (25, 31). All animal handling was approved by the ethics committee of the University of Barcelona in accordance with EU regulations.

DNA Synthesis—DNA synthesis was measured as the incorporation of [^{3}H]thymidine (Amersham Biosciences) to DNA, as described elsewhere (22). Briefly, macrophages (5×10^4) were seeded in 24-well plates in 1 ml of medium without M-CSF for at least 18 h. Cells were then cultured for a further 24 h in the absence or presence of M-CSF with/without LPS, TNF-α, MgTx, or $BaCl_2$ (1 mM). Finally, the medium was removed and replaced with 0.5 ml of the same medium containing 1 μCi/ml [^{3}H]thymidine. After three additional hours of incubation, cells were fixed in 70% methanol, washed three times in ice-cold 10% trichloroacetic acid, and solubilized in 1% SDS and 0.3% NaOH. The whole content of the well was used for counting radioactivity.

RNA Isolation and RT-PCR Analysis—Total RNA from mouse macrophages, brain, and liver was isolated using the Tripure reagent (Roche Diagnostics), following the manufacturer's instructions. Samples were further treated with the DNA-free kit from Ambion Inc. to remove DNA.

Ready-to-Go RT-PCR beads (Amersham Biosciences) were used in a one-step RT-PCR as described elsewhere (22, 32–34). Total RNA and selected primers at 1 μM were added to the beads. The RT reaction was initiated by incubating the mixture at 42 °C for 30 min. Once the first-strand cDNA had been synthesized, the conditions were set for further PCR: 92 °C for 30 s, either 55 °C (Kv1.3 and 18S) or 60 °C (Kir2.1) for 1 min and 72 °C for 2 min. These settings were applied for 40 cycles. Every 10 cycles, 10 μl of the total reaction was collected in a separate tube for further electrophoresis and analysis. A range of dilutions of RNA from each independent sample was performed to obtain an exponential phase of amplicon production (not shown) as described previously (32). The same independent RNA aliquot was used to analyze the VDPC mRNA expression and the respective amount of 18 S rRNA. Primer sequences and accession numbers were: Kv1.3 (accession number M30441), forward, 5′-CTCATCTCCATTGTCATCTTCTGA-3′ (base pairs 741–765) and reverse, 5′-TTGAATTGGAAACAATCAC-3′ (base pairs 1459–1440); Kir2.1 (accession number AF021136), forward, 5′-TGGCTGTGTGTTTTGGTTGATAGC-3′ (base pairs 297–320) and reverse, 5′-CTTTGCCATCTTCGCCATGACTGC-3′ (base pairs 555–532); and 18 S (accession number X00686), forward, 5′-CGCAGAATTCCCA-CTCCCGACCC-3′ (base pairs 482–498) and reverse, 5′-CCCAAGCTC-CAACTACGAGC-3′ (base pairs 694–675). Kv1.5 and other Kv mRNA expression was analyzed by PCR as previously described (33). In all cases negative controls were performed in the absence of the RT reaction.

Once the exponential phase of the amplicon production had been determined the specificity of each product was confirmed in test RT-PCR using the appropriate cDNA probe in a Southern blot analysis. PCR-generated VDPC cDNA probes from mouse brain were subcloned using the pSTBlue-1 acceptor vector kit (Novagen) and the sequences were confirmed using the Big Dye Terminator Cycle sequencing kit and an ABI 377 sequencer (Applied Biosystems). EcoRI-digested [α-^{32}P]CTP random primer-labeled cDNAs were used as probes as previously described (34). At least three different filters were made from independent samples and representative blots are shown. Results were analyzed with Phoretix software (Nonlinear Dynamics).

Protein Extracts and Western Blot—Cells were washed twice in cold phosphate-buffered saline (PBS) and lysed on ice with lysis solution (1% Nonidet P-40, 10% glycerol, 50 mmol/liter HEPES, pH 7.5, 150 mmol/liter NaCl) supplemented with 1 μg/ml aprotinin, 1 μg/ml leupeptin, 86 μg/ml iodoacetamide, and 1 mM phenylmethylsulfonyl fluoride as protease inhibitors. Sample protein concentration was determined by Bio-Rad protein assay. The proteins from cell lysates (100 μg) were boiled at 95 °C in Laemmli SDS-loading buffer and separated on 10% SDS-PAGE. They were transferred to nitrocellulose membranes (Immobilon-P, Millipore), and blocked in 5% dry milk-supplemented 0.2% Tween 20 PBS prior to immunoreaction. To monitor Kv1.3 and Kir2.1 expression, rabbit polyclonal antibodies (Alomone Labs) were used. To study the expression of inducible nitric-oxide synthase (iNOS), a rabbit antibody against mouse iNOS (Santa Cruz Biotechnology) was used. The rabbit polyclonal anti-Kv1.5 antibody was a kind gift from Dr. M. M. Tamkun (Colorado State University). As a loading and transfer control, a monoclonal anti-β-actin antibody (Sigma) was used.

Electron Microscopy—Cell monolayers on Petri dishes were scraped and collected into PBS buffer. BMDM were cryofixed by high-pressure freezing using an EMPact (Leica). Freeze substitution was performed in an "Automatic Freeze Substitution system" (AFS) from Leica, using acetone containing 0.5% of uranyl acetate, for 3 days at −90 °C. On the fourth day, the temperature was slowly increased, 5 °C/h, to −50 °C. At this temperature samples were rinsed in acetone and then infiltrated and embedded in Lowicryl HM20. Ultrathin sections were picked up on Formvar-coated copper-palladium grids. For immunogold localization, samples were blocked with 10% fetal calf serum in PBS for 20 min and incubated at room temperature for 1 h with polyclonal anti-Kv1.3 or anti-Kir2.1 (1:200). Washes were performed with PBS prior to adding goat anti-rabbit conjugated to 10 nm colloidal gold (BioCell Research Laboratory) for 1 h at room temperature. Finally, samples were washed and contrasted with 2% uranyl acetate for 30 min and observed in a Hitachi 600AB electron microscope.

Electrophysiological Recordings—Whole cell currents were measured using the patch clamp technique. An EPC-9 (HEKA) with the appropriate software was used for data recording and analysis. Currents were filtered at 2.9 kHz. Series resistance compensation was always above 70%. Patch electrodes of 2–4 Mohms were fabricated in a P-97 puller (Sutter Instruments Co.) from borosilicate glass (outer diameter 1.2 mm and inner diameter 0.94 mm; Clark Electromedical Instruments Co.). Electrodes were filled with the following solution (in mM): 120 KCl, 1 $CaCl_2$, 2 $MgCl_2$, 10 HEPES, 11 EGTA, 20 D-glucose, adjusted to pH 7.3 with KOH. The extracellular solution contained (in mM): 120 NaCl, 5.4 KCl, 2 $CaCl_2$, 1 $MgCl_2$, 10 HEPES, 25 D-glucose, adjusted to pH 7.4 with NaOH. After establishing the whole cell configuration of the patch clamp technique macrophages were clamped to

were held at −60 mV and pulse potentials as described in the legend to Fig. 1 were applied. Conductance was plotted against test potentials. *C*, steady-state activation curves of the outward current. Conductance above holding potentials were normalized to the peak current density at +50 mV. *D*, steady-state activation curves of the inwardly rectifying current. Conductance below holding potentials were normalized to the current density at −150 mV. Symbols for *B–D panels* are: ○, −M-CSF; ●, +M-CSF. *E*, Kv1.3 and Kir2.1 mRNA expression. Samples were collected after the addition of M-CSF and RT-PCR analysis was performed as described under "Experimental Procedures" at the indicated times. Values are the mean ± S.E. ($n = 4$). Significant differences were found with Kv1.3 and Kir2.1 ($p < 0.001$, ANOVA). *F*, Kv1.3 and Kir2.1 protein expression in BMDM cultured during 24 h in the absence (−) or presence (+) of M-CSF.

a holding potential of −60 mV. To evoke voltage-gated currents all cells were stimulated with 200-ms square pulses ranging from −150 to +50 mV in 10-mV steps. All recordings were routinely subtracted for leak currents.

The pharmacological characterization of the inward rectifier K^+ current was performed by adding to the external solution $BaCl_2$ and CsCl at various concentrations (28). To block the outward current, MgTx and ShK-Dap^{22} were added to the external solution (26, 27). Before experiments, toxins were reconstituted to 10 μM in Tris buffer (0.1% bovine serum albumin, 100 mM NaCl, 10 mM Tris, pH 7.5). All recordings were done at room temperature (20–23 °C).

Reagents—Recombinant murine TNF-α was obtained from Prepo-Tech EC. Recombinant murine M-CSF was from R&D Systems. Cycloheximide, actinomycin D, LPS, CsCl, and $BaCl_2$ were purchased from Sigma, and MgTx from Alomone Labs. ShK-Dap^{22} was from Bachem Biosciences Inc. Other reagents were of analytical grade.

Analysis and Statistics—According to the solutions used, the calculated equilibrium potential for potassium was −79 mV (E_K) using the Nernst equation. The normalized G/G_{max} *versus* voltage curve was fitted using Boltzmann's equation: $G/G_{max} = 1/(1 + \exp^{((V[1,2]-V)/k)})$, where $V_{½}$ is the voltage at which the current is half-activated and k is the slope factor of the activation curve.

Values are expressed as the mean ± S.E. The significance of differences was established by either Student's t test or one way ANOVA (Graph Pad, PRISM 3.0) for either two-group or two-factor comparison, respectively. A value of $p < 0.05$ was considered significant.

RESULTS

Macrophages Express Outward and Inward K^+ Currents: Pharmacology and Molecular Characterization of Kv1.3 and Kir2.1—Cells (n = 80) plated in the presence in L-cell-conditioned medium expressed outward delayed and inward rectifier potassium currents (Fig. 1*A*). Following a train of 200-ms depolarizing pulses to +50 mV at 400-ms intervals, the outward current showed a characteristic cumulative inactivation phenomenon (Fig. 1*B*). Fig. 1*C* shows the effect of MgTx and ShK-Dap^{22} on the outward conductance. The IC_{50} for inhibition were ~5 and ~3 pM for MgTx and ShK-Dap^{22}, respectively. These results indicated that Kv1.3 would be the main channel responsible for the outward potassium current. On the other hand, the high sensitivity to Ba^{2+} (Fig. 1*D*) and Cs^+ (Fig. 1*E*), together with the closed state above 0 mV of the inward current, indicated that the channel was Kir2.1. To identify K^+ channels at the molecular level, we performed RT-PCR analyses. Mouse brain and liver RNAs were used as positive and negative controls, respectively. Fig. 2*A* shows that macrophages expressed Kv1.3 and Kir2.1 mRNA to a similar extent to that observed in the brain. In addition, specific Kv1.3 and Kir2.1 signals were obtained by Western blot analysis in brain and BMDM protein samples (Fig. 2*B*). The presence of other VDPC (Kv1.1, Kv1.2, Kv1.6, and Kv3.1) analyzed by RT-PCR was negative (Fig. 2*C*). However, BMDM expressed Kv1.5 mRNA but the protein expression was below detection levels analyzed by Western blot (Fig. 2*C* and data not shown).

The expression of Kv1.3 and Kir2.1 proteins in macrophages was further confirmed by electron microscopic immunocytochemical detection studies with specific antibodies (Fig. 2, *D* and *E*, respectively). Taken together, these data indicate that BMDM have outward delayed and inward rectifier potassium currents that are mainly conducted by Kv1.3 and Kir2.1 K^+ channels.

M-CSF-dependent Proliferation Induces Kv1.3 and Kir2.1—M-CSF is the specific growth factor for this cell type. Macrophages incubated for about 18 h in the absence of this factor stopped cell growth (>98%) and became quiescent (22). The addition of M-CSF triggered macrophage proliferation (not shown) and outward and inward K^+ currents were induced after 24 h of incubation (Fig. 3*A*). The current density (pA/pF)/voltage relationships depicted in Fig. 3*B* showed that M-CSF increased currents up to 3-fold. The number and density of the channels were increased during M-CSF-dependent proliferation. Whereas at +50 mV resting cells expressed ~30 channels/cell with a density of ~0.017 channel/μm^2, proliferating cells showed ~90 channels/cell and ~0.05 channel/μm^2. A large increase was also observed in the inward current at −150 mV. Thus, M-CSF-treated macrophages increased from ~80 to ~275 channels/cell and from ~0.044 to ~0.15 channel/μm^2 for the number and channel density, respectively. Normalized conductance demonstrated that both groups showed similar patterns. Thus, outward currents (Fig. 3*C*) indicated that channels were open at depolarizing potentials with a $V_{½}$ of −10.53 ± 2.8 and −11.33 ± 2.1 mV and k of 20 ± 3 and 21 ± 3 for resting (−M-CSF) and proliferating (+M-CSF) cells, respectively (n = 20). Moreover, the steady-state activation of inward currents (Fig. 3*D*) was also similar, with $V_{½}$ values of −105 ± 2 and −109 ± 2 mV and slopes k of −12.0 ± 1 and −12.4 ± 1 for −M-CSF and +M-CSF cells, respectively (n = 20).

Fig. 3*E* illustrates the time course of Kv1.3 and Kir2.1 gene expression after the addition of M-CSF. The expression of both VDPC increased by up to 3-fold. However, whereas Kv1.3 reached the highest levels after about 6 h, Kir2.1 expression increased steadily throughout the study. Similar changes were obtained in Kv1.3 and Kir2.1 protein abundance in BMDM incubated during 24 h in the presence of M-CSF (Fig. 3*F*). No differences were observed in the absence of M-CSF throughout the study. Taken together, these data indicate that M-CSF-dependent proliferation leads to long term increases in current densities of outward and inward currents in accordance with an induction in mRNA and protein expression.

LPS-induced Activation Regulates Differentially Kv1.3 and Kir2.1—Proliferating macrophages reach body tissues and are activated by physiological processes. The addition of LPS for 24 h in the presence of M-CSF inhibited proliferation (99.5 ± 0.5%, n = 12). LPS also increased the outward current concomitantly to a reduction in the inward current (Fig. 4*A*). The current density/voltage relationship depicted in Fig. 4*B* indicates that at depolarizing potentials the current was increased 4-fold, whereas at hyperpolarizing potentials the inward current was reduced about 5-fold. Thus, in the presence of LPS the number of the outward delayed rectifier functional channels and their density was 5 times larger that in its absence at +50 mV (~90 and ~420 channels/cell and ~0.05 and ~0.25 channel/μm^2, respectively). On the contrary, at −150 mV, the number and density of the inward channels decreased, being ~40 and ~275 channels/cell and ~0.022 and ~0.15 channel/μm^2 for LPS-treated and untreated macrophages, respectively. In the presence of 10 nM MgTx outward currents were totally inhibited, with no effect on the inward conductance (Fig. 4*C*). Fig. 4*D* shows the steady-state activation curves of the normalized outward current above the holding potential. Whereas $V_{½}$ values were similar for both groups (−12.8 ± 1.1 and −15.7 ± 3.6 mV for −LPS and +LPS, respectively, n = 10), k slope values were significantly different (21.0 ± 3 and 9.3 ± 1.2 for −LPS and +LPS, respectively, $p < 0.001$, n = 10). However, when the steady-state activation curves of inward currents were analyzed (Fig. 4*E*), both groups showed similar characteristics. Thus, $V_{½}$ values were −108 ± 2 and −105.8 ± 1 mV and k values were −12.6 ± 1 and −11.9 ± 1 for −LPS and +LPS, respectively (n = 10).

Fig. 5 shows Kv1.3 and Kir2.1 expression in the presence of M-CSF with or without LPS at different times. The presence of LPS induced the expression of Kv1.3 mRNA about 4-fold after 3 h (Fig. 5*A*). After 24 h, Kv1.3 mRNA still was ~275% above control. In contrast, Kir2.1 mRNA decreased steadily. Fig. 5*B* shows that the mRNA regulation observed for Kv1.3 and Kir2.1 was mirrored by similar changes in protein expression levels.

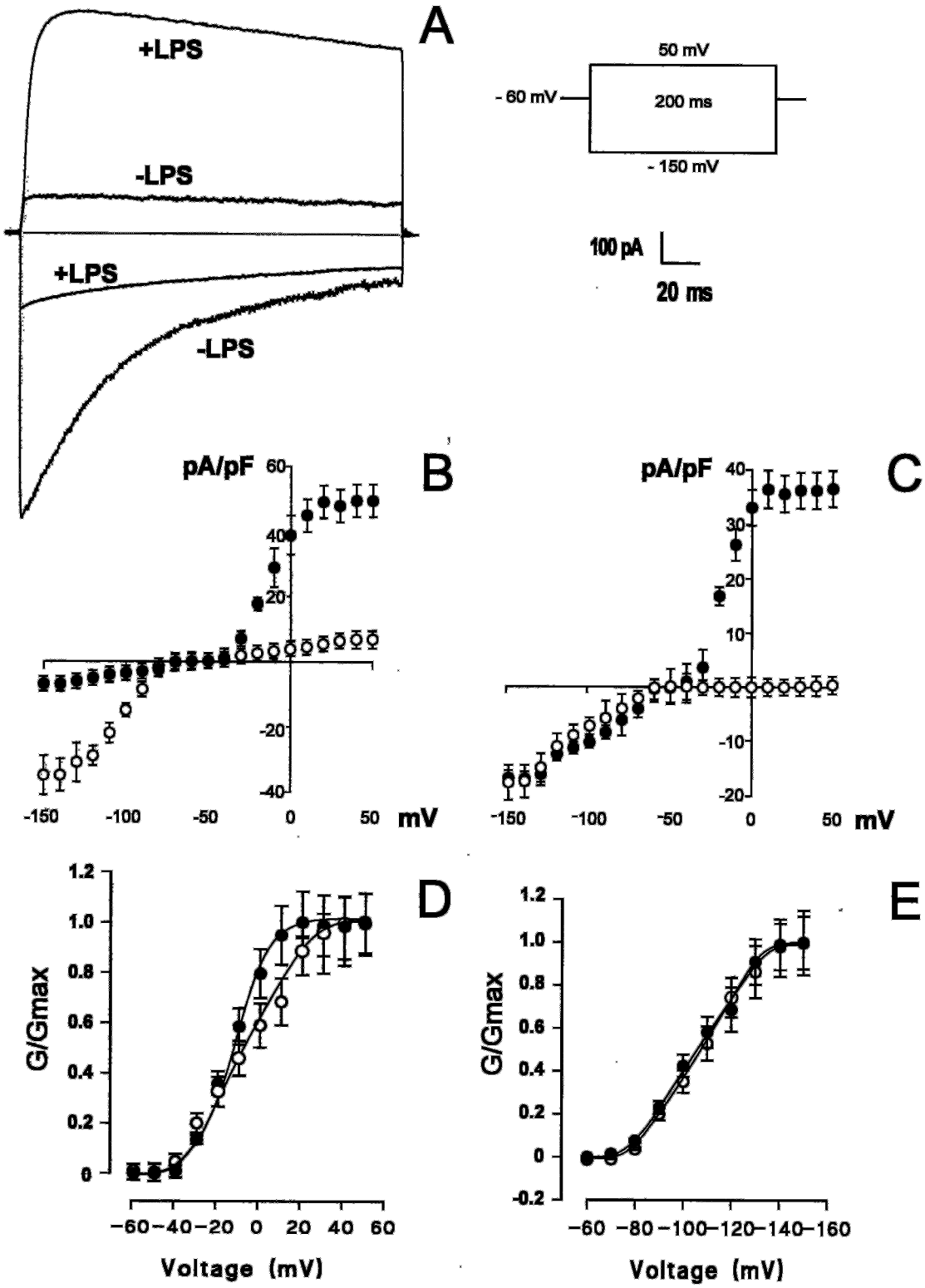

FIG. 4. **LPS-induced activation regulates K^+ currents differentially in macrophages.** BMDM were incubated with M-CSF for 24 h in the presence (+*LPS*) or absence (−*LPS*) of the endotoxin. *A*, representative outward and inward traces were elicited as indicated. *B*, current density *versus* voltage representation of K^+ currents. Macrophages were held at −60 mV and pulse potentials were applied as indicated in the legend to Fig. 1. *C*, current density/voltage relationship of the specific inhibition of outward K^+ currents by 10 nM MgTx. Cells were treated with LPS and currents were evoked in the presence (○) or absence (●) of MgTx. Pulse potentials were applied as indicated in the legend to Fig. 1. *D*, steady-state activation curve of the outward current. Conductance *above* the holding potentials were normalized to the peak current density at +50 mV. *E*, steady-state activation curves of the inwardly rectifying current. Conductance *below* the holding potentials were normalized to the peak current density at −150 mV. Symbols for *B–E panels*: ○, −LPS; ●, +LPS. Values are the mean ± S.E. (n = 10).

TNF-α Regulates Kv1.3 and Kir2.1 Similarly to LPS, Evidence for LPS Modulation by TNF-α-dependent and -independent Mechanisms—TNF-α produced by macrophages and lymphocytes mediates a number of events induced by LPS, including activation, apoptosis, and the nucleoside uptake (25, 35). To examine whether TNF-α mediates LPS regulation of

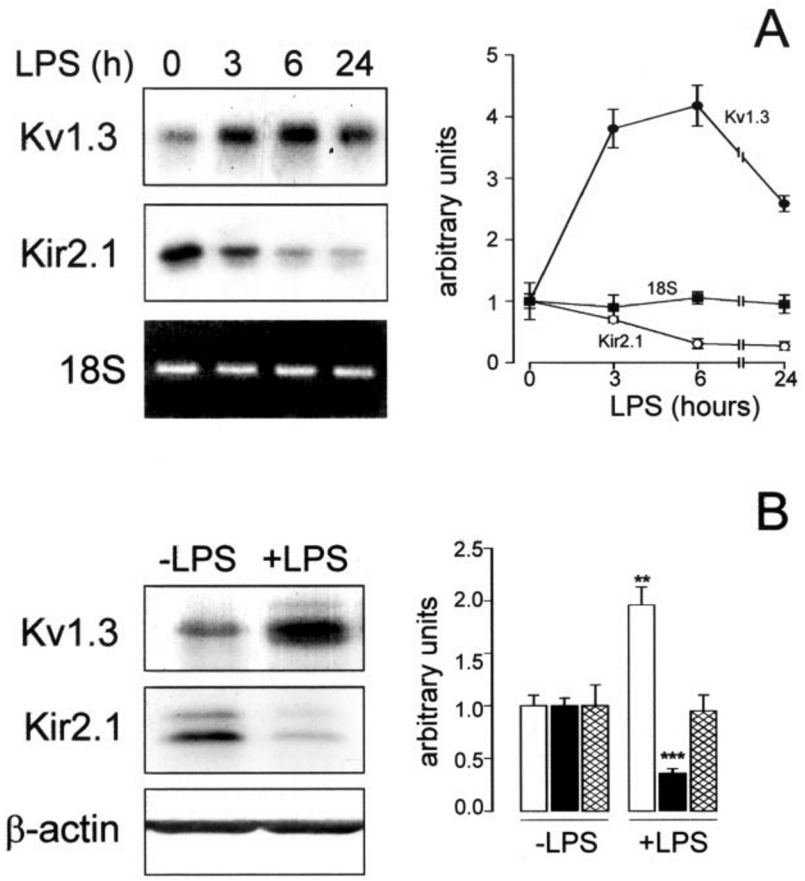

FIG. 5. **LPS-induced activation up-regulates Kv1.3 and down-regulates Kir2.1 VDPC.** *A*, RT-PCR analysis of Kv1.3 and Kir2.1 mRNA expression at different times after LPS treatment. Results from RT-PCR on 0.25 μg of total RNA for 30 cycles for Kv1.3 and Kir2.1 and 0.1 μg of RNA and 10 cycles for 18 S are shown. These conditions were at the exponential phase of the amplicon production as described under "Experimental Procedures." ●, Kv1.3; ○, Kir2.1; ■, 18 S. Significant differences were found with Kv1.3 and Kir2.1 ($p < 0.001$, ANOVA). *B*, Kv1.3 and Kir2.1 Western blot analysis. Cells were incubated for 24 h with (+*LPS*) or without (−*LPS*) the endotoxin. *Open bars*, Kv1.3; *closed bars*, Kir2.1; *hatched bars*, β-actin. **, $p < 0.01$; ***, $p < 0.001$ *versus* −LPS (Student's *t* test). Representative filters are shown. Values are mean ± S.E. of four independent experiments.

VDPC, macrophages in the presence of M-CSF were incubated for 24 h with (+TNF-α) or without (−TNF-α) TNF-α, and K^+ currents were analyzed (Fig. 6). The cytokine increased the outward current and decreased the inward (Fig. 6*A*). Current density/voltage relationships (Fig. 6*B*) demonstrated that at depolarizing potentials the outward current was 3-fold induced while at hyperpolarizing potentials the inward was 6-fold lower. In addition, at a potential of +50 mV, there was a considerable increase in the number and density of outward channels (~90 and ~240 channels/cell; ~0.15 and ~0.22 channel/μm^2 for TNF-α untreated and treated cells, respectively), at −150 mV the number and density of the inward ones was lower (~275 and ~40 channels/cell; ~0.15 and ~0.022 channel/μm^2). The steady-state activation curves for outward and inward currents are shown in Fig. 6, *C* and *D*, respectively. Outward current $V_{½}$ values were similar for both groups (−13.1 ± 2.7 and −17.0 ± 2.0 mV for −TNF-α and +TNF-α, respectively, $n = 9$). However, k slope values were different (21.0 ± 3 and 9.8 ± 1 for −TNF-α and +TNF-α, respectively, $p < 0.001$, $n = 9$). Inward currents were similar (Fig. 6*D*), with $V_{½}$ values −107.6 ± 2 and −107.9 ± 2 mV, and k values −16.7 ± 1.3 and −18.8 ± 1.5 for −TNF-α and +TNF-α, respectively ($n = 9$).

The expression of Kv1.3 and Kir2.1 mRNA and protein was also analyzed (Fig. 7). Kv1.3 mRNA induction peaked (~3-fold) after 3 h of incubation (Fig. 7*A*) and remained high throughout the study. Kir2.1 mRNA expression decreased for the first 6 h and remained low (about 30% of basal) for a further 24 h. Similarly to what was found with the mRNA, VDPC protein abundance was differentially regulated (Fig. 7*B*). Thus, whereas Kv1.3 showed a significant increase (~180%) after 24 h, Kir2.1 protein expression decreased about 50%.

To further explore the role of TNF-α in the LPS signaling, we used BMDM from TNF-α receptor I/II double knockout mice. As expected, TNF-α triggered Kv1.3 up-regulation and Kir2.1 down-regulation only in wild type (+/+) but not in TNF-α receptor I/II double knockout (−/−) cells (Fig. 8, *C* and *D*). Interestingly, LPS induced Kv1.3 and down-regulated Kir2.1 in both groups (Fig. 8, *A* and *B*). Taken together, these results indicate that although the autocrine production of TNF-α regulates VDPC similarly to LPS, redundant pathways must be involved.

Macrophage Proliferation and Activation Require VDPC Expression—Proliferation induced outward and inward K^+ currents in macrophages. However, LPS and TNF-α triggered an induction of the outward current, whereas the inward current decreased (Fig. 9*A*). Concomitantly, the mRNA and protein expression of both VDPC were regulated differentially. Ion channels are under extensive regulation, and changes among different expression levels have been reported. However, in long term studies, VDPC mRNA mostly governs protein and activity (13, 34, 36). The regulation of K^+ currents was dependent on mRNA and protein *de novo* synthesis because it was prevented by the presence of either actinomycin D or cycloheximide (Fig. 9*A*). To examine whether other VDPC, besides Kv1.3, were involved in the M-CSF-dependent proliferation and LPS- or TNF-α-induced activation, currents were evoked in the presence or absence of MgTx (Fig. 9*B*) and ShK-Dap^{22} (Fig. 9*C*). Similar results were obtained in all conditions, indicating that Kv1.3 is the main channel responsible for the outward currents. However, because Kv1.5 mRNA was detected in BMDM by RT-PCR, we analyzed its expression in macrophages cultured under distinct stimuli (Fig. 9*D*). Neither M-CSF-dependent proliferation nor LPS- and TNF-α-induced activation regulated Kv1.5 mRNA expression.

To further analyze the physiological role of VDPC during macrophage proliferation, cells were incubated for 24 h in the presence of M-CSF with or without MgTx and Ba^{2+}. The addition of MgTx inhibited BMDM proliferation in a dose-dependent man-

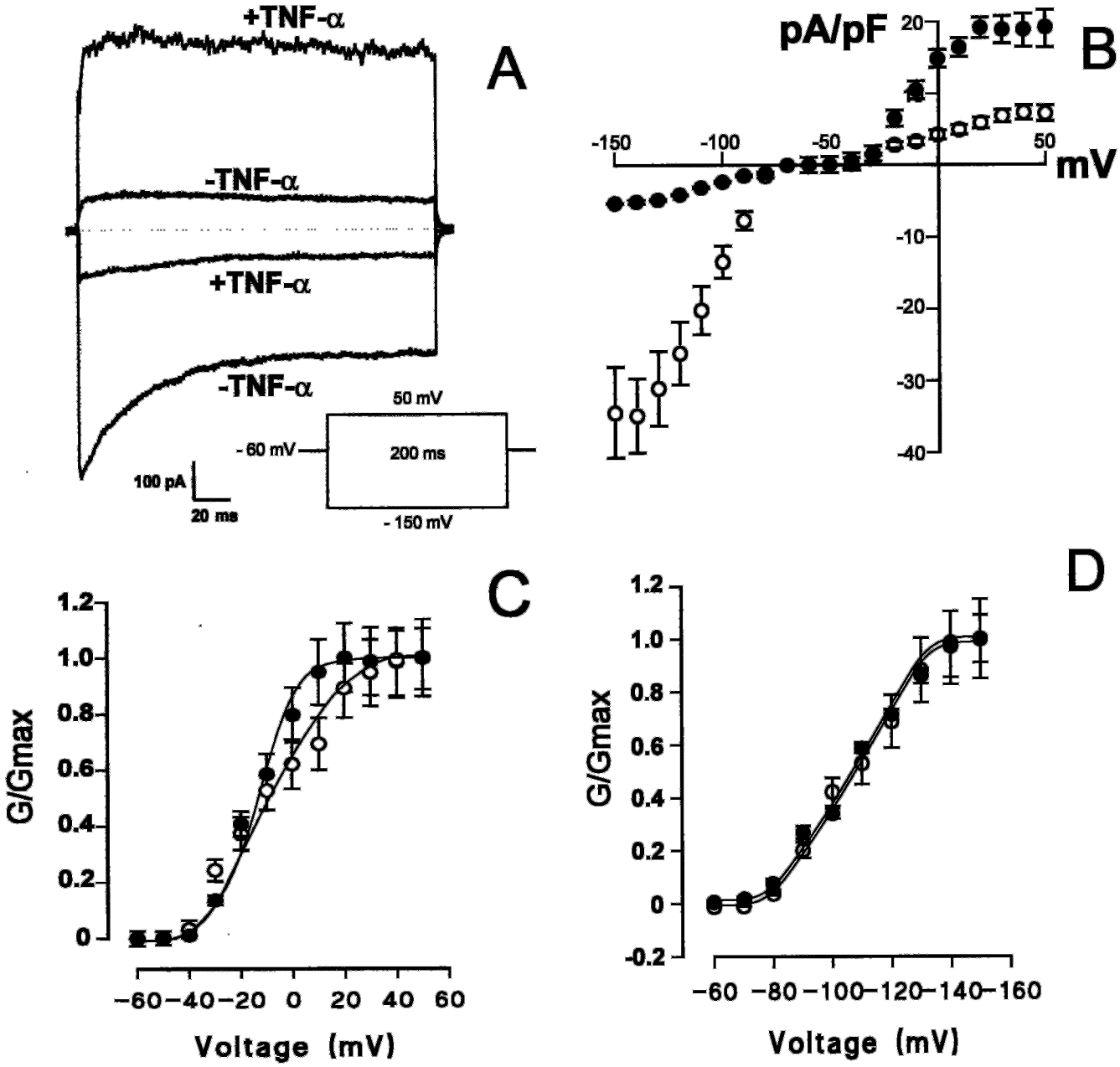

FIG. 6. **TNF-α regulates K^+ currents differentially in macrophages.** BMDM were incubated with M-CSF for 24 h in the presence (+*TNF-α*) or absence (−*TNF-α*) of the cytokine. *A*, representative outward and inward traces were elicited as indicated. *B*, current density/voltage relationship of K^+ currents. Cells were held at −60 mV and pulse potentials were applied as indicated in the legend to Fig. 1. *C*, steady-state activation curves of the outward current. Conductance above holding potentials were normalized to the peak current at +50 mV. *D*, steady-state activation curves of the inwardly rectifying current. Conductance *below* the holding potentials were normalized to the peak current at −150 mV. ○, −TNF-α; ●, TNF-α. Values are the mean ± S.E. (n = 9).

ner with a IC_{50} of 2.2 nM (Fig. 9*E*). Moreover, cell growth was also lower in the presence of 1 mM Ba^{2+} (52 ± 6%, n = 9) and the addition of 10 nM MgTx further inhibited [^{3}H]thymidine incorporation (69 ± 4%, $n = 6, p < 0.05$ *versus* 1 mM Ba^{2+} or 10 nM MgTx alone). These results indicate that Kv1.3 and Kir2.1 could be involved in the BMDM proliferation in an additive way.

The role of TNF-α in the LPS-induced activation seems to be partial, because not only the outward K^+ current but also the proliferation were modulated to a lesser extent by TNF-α. Thus, while LPS totally abolished cell growth (see above), the inhibition of [^{3}H]thymidine incorporation in the presence of TNF-α was 61 ± 5%. In addition, the pharmacological blockage of VDPC was additive, because proliferation was further decreased when either 10 nM MgTx or 1 mM Ba^{2+} was added to TNF-α (91 ± 10 and 80 ± 4%, respectively, n = 6, $p < 0.001$ *versus* TNF-α alone).

The potential role of VDPC during proliferation and activation was further supported by the effects of MgTx on iNOS expression in BMDM (Fig. 9*F*). iNOS is dependent on K^+ channel activity in macrophage-like cell lines (37), and similarly to IL-2 in T-cell (38), could be considered as a marker of macrophage activation (25, 35). LPS and TNF-α-induced activation triggered an increase in iNOS expression and the presence of 10 nM MgTx inhibited iNOS induction (Fig. 9*F*).

DISCUSSION

Since the early 1980s several laboratories have been characterizing ion channels in red blood cells and leukocytes. Several

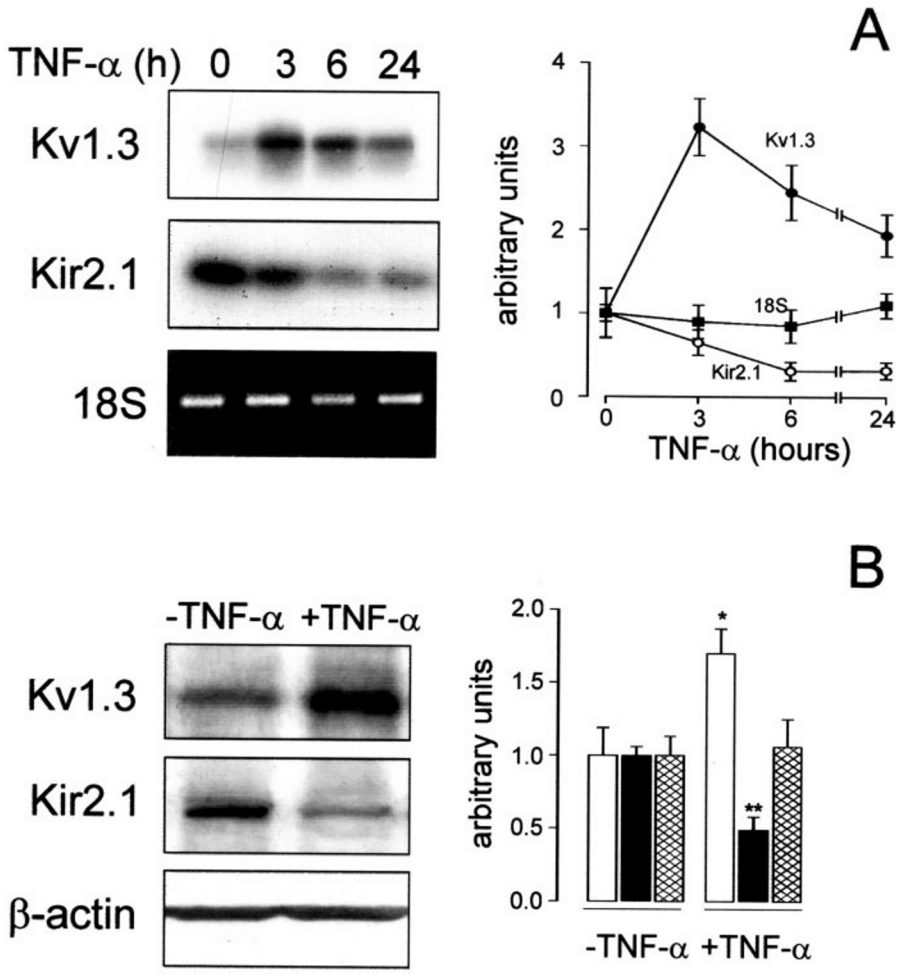

FIG. 7. **TNF-α up-regulates Kv1.3 and down-regulates Kir2.1 VDPC.** *A*, RT-PCR analysis of Kv1.3 and Kir2.1 mRNA expression at different times after TNF-α treatment. Results from RT-PCR on 0.25 μg of total RNA during 30 cycles for Kv1.3 and Kir2.1 and 0.1 μg of RNA and 10 cycles for 18 S are shown. These conditions were at the exponential phase of the amplicon production as described under "Experimental Procedures." ●, Kv1.3; ○, Kir2.1; ■, 18 S. Significant differences were found with Kv1.3 and Kir2.1 ($p < 0.001$, ANOVA). *B*, Kv1.3 and Kir2.1 Western blot analysis. Cells were incubated for 24 h with (+*TNF-α*) or without (−*TNF-α*) the cytokine. *Open bars*, Kv1.3; *closed bars*, Kir2.1; *hatched bars*, β-actin. *, $p < 0.05$; **, $p < 0.01$ *versus* −TNF-α (Student's *t* test). Representative filters are shown. Values are mean ± S.E. of four independent experiments.

types of voltage-dependent sodium, chloride, proton, and potassium currents have been identified in macrophages of diverse origin. Among them, voltage-gated outward and inward K^+ currents have been the most studied. In leukocytes, whereas outward K^+ currents contribute to restoring membrane potential after depolarization, inward K^+ currents have a key role after hyperpolarization (see Refs. 18–20 and 37 for reviews).

Voltage-dependent K^+ Channels in Bone Marrow-derived Macrophages—The present study identifies for the first time the VDPC expressed in non-transformed macrophages. BMDM is a cell model that follows the physiological schedule within the body (2, 22, 25). Mature cells may proliferate or become activated after a specific stimulus. The use of dedifferentiated cell lines (THP-1 or HL-60 among others) as well as thioglycollate-elicited peritoneal macrophages, blood monocytes, or microglia has yielded controversial results (4–20, 39–42). Those data imply that K^+ channels expressed in macrophages depend on the source and the differentiated status of the cells. Furthermore, the presence of K^+ currents in BMDM had been reported but the proteins responsible had not been identified (42). Our results indicate that Kv1.3 is the main channel responsible for the outward current and Kir2.1 is responsible for the inward.

The presence of other candidates was tested in our model. Lymphocytes express several voltage-dependent K^+ currents (*n, n′*, and *l*-type channels). While Kv1.3 is associated with the *n*-type channel and Kv3.1 accounts for the *l*-type, the protein responsible for the *n′*-type is unknown (38). In addition, other channels have been described in immune system cells. Thus, KCNE1 (also named Isk) was cloned from T-cells (43), Kv1.1 was found in $CD4^-CD8^-$ thymocytes (44) and Kv1.5 was identified in non-proliferating hippocampal microglia (45). We did not find Kv3.1 and Kv1.1 in macrophages by RT-PCR. Other related Kv1 channels such as Kv1.2 and Kv1.6 were also absent in our model. This result is consistent with the specific blockage of the outward current by MgTx and ShK-Dap[22], even when cells proliferated or were activated. However, the expression of Kv1.5 indicates that heterotetrameric structures between Kv1.3 and Kv1.5 would be possible and should be considered.

M-CSF-dependent Proliferation Versus LPS-induced Activation—VDPC are implicated in proliferation and activation. Their role in G_1/S cell cycle progression has been reviewed, and their function in IL-2 secretion by T-lymphocytes has been demonstrated (38). However, different cell models produce controversial results. Whereas in some cell lines the differentiation is a prerequisite for VDPC expression, the macrophage phenotype often determines the loss of specific ion channel properties (18). Many studies have used B- and T-cells. However, lymphocyte activation leads to associated proliferation via autocrine production of IL-2 (38). In this cellular scenario, the physiological role of VDPC in the immune system remains to be determined.

We have found that M-CSF-dependent proliferation led to an increase in the K^+ current conducted by Kv1.3. Links between proliferation and VDPC expression are supported by the cell growth arrest in the presence of K^+ channel blockers (36, 46, this study). M-CSF activates phosphorylation cascades that involve Src homology 2 domains and induction of mitogen-activated protein kinase (24). Kv1.3 shows tyrosine kinase regulation and, in addition to its role as an ion channel, might be involved in the activation of Src-like tyrosine kinases that

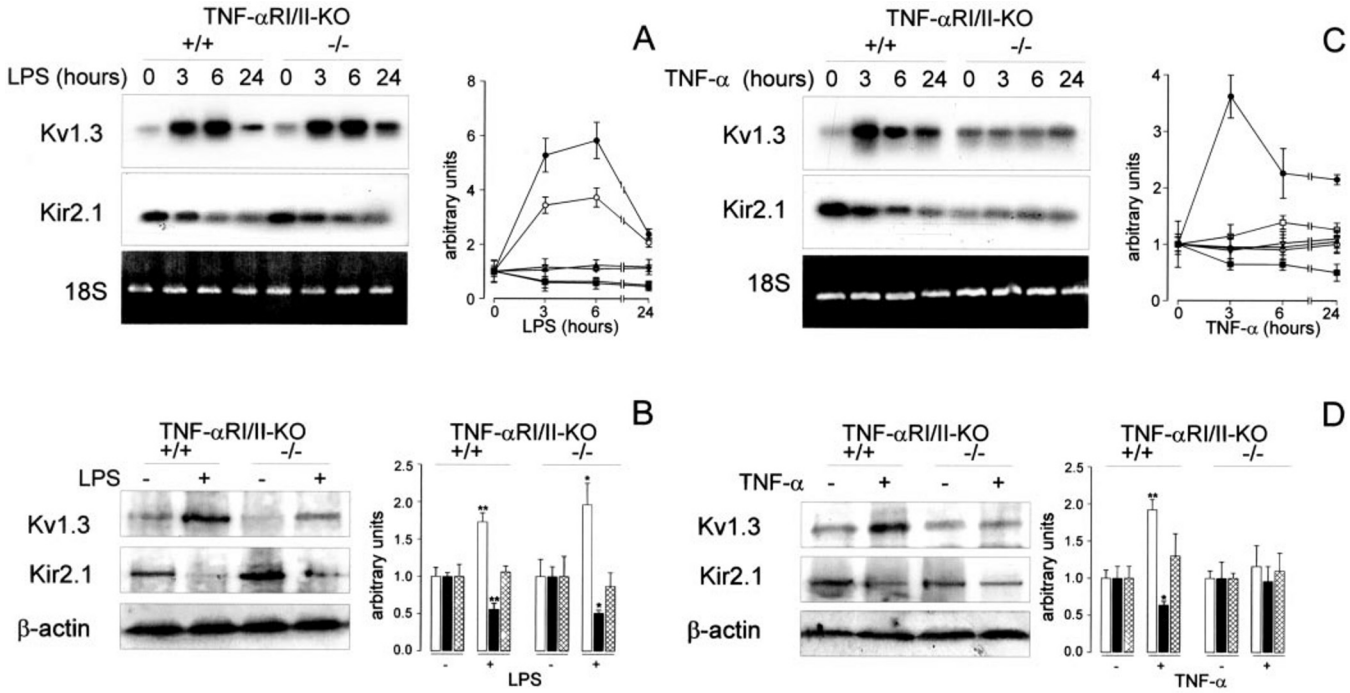

FIG. 8. **Evidence for TNF-α-independent mechanisms mediating the VDPC regulatory responses to LPS in macrophages.** Cells cultured in the absence of M-CSF for 18 h were incubated for a further 24 h in the presence of the growth factor supplemented with LPS or TNF-α. Samples from wild type (+/+) or TNF-α receptor I/II double knockout (−/−) mice were collected at the indicated times. *A*, RT-PCR analysis of Kv1.3 and Kir2.1 mRNA expression after LPS treatment. RT-PCR results were at the exponential phase of the amplicon production as described in the legend to Fig. 5. Significant differences were found in Kv1.3 and Kir2.1 ($p < 0.001$, ANOVA). ●, ○: Kv1.3; ■, □: Kir2.1; ▲, △: 18 S. *Closed symbols*, +/+; *open symbols*, −/−. *B*, Kv1.3 and Kir2.1 Western blot analysis. Cells were incubated for 24 h with (+*LPS*) or without (−*LPS*) the endotoxin. *Open bars*, Kv1.3; *closed bars*, Kir2.1; *hatched bars*, β-actin. *, $p < 0.05$; **, $p < 0.01$ *versus* −LPS (Student's *t* test). *C*, RT-PCR analysis of Kv1.3 and Kir2.1 mRNA expression after TNF-α treatment. RT-PCR results were at the exponential phase of the amplicon production as described in the legend to Fig. 7. *Symbols* are described in *A*. Kv1.3 and Kir2.1 significant differences were found only in +/+ macrophages ($p < 0.001$, ANOVA). *D*, Kv1.3 and Kir2.1 Western blot analysis. Cells were incubated for 24 h with (+*TNF*-α) or without (−*TNF*-α) the cytokine. Symbols are described in *B*. *, $p < 0.05$; **, $p < 0.01$ *versus* −TNF-α (Student's *t* test). Representative filters are shown. Values are mean ± S.E. of four independent experiments.

are important for cell growth (47, 48). However, our results go further, because we demonstrate that the long term increase in Kv1.3 activity is under *de novo* mRNA and protein synthesis, similarly to what was observed with the inward K^+ current and Kir2.1. This is in contrast to what is described in phorbol 12-myristate 13-acetate-differentiated HL-60 cells or thioglycollate-elicited peritoneal macrophages (12). However, our results are in agreement with studies in which Ba^{2+} inhibits melanoma cell proliferation linked to a decrease in the membrane depolarization (28).

The question arises as to why macrophages need both K^+ channels to proliferate. Whereas the Kv1.3 current could set the membrane potential at −50 to −60 mV, Kir2.1 would shift the potential to more negative values, close to the Nernst potassium equilibrium. A similar mechanism operates during myogenesis. Kir2.1 forces the potential to more negative values than hERG channels, leading to cell fusion mediated by Ca^{2+} (49). The degree of membrane hyperpolarization determines the extent of Ca^{2+} influx (49, 50). In macrophages, MgTx and Ba^{2+} inhibited proliferation and their combination was additive. In addition, MgTx and Ba^{2+} partially block proliferation in oligodendrocytes and melanoma cells (28, 36). These results have physiological significance because an increase in intracellular Ca^{2+} activates calcineurin, the translocator of the transcriptional factor NF-IL2A, the mitogen-activated protein II kinase, and the DNA synthesis promoting factor (38, 51). Consequently, by inducing Kv1.3 and Kir2.1, macrophages would maintain sufficiently negative potential to open Ca^{2+} channels and thus initiate mitotic Ca^{2+} signaling pathways.

LPS-induced activation blocks macrophage proliferation (25, 35) and regulates Kv1.3 and Kir2.1 under mRNA and protein synthesis control. Previous studies show that K^+ currents can be differentially regulated. Whereas granulocyte macrophage-CSF and LPS induce the outward current, without changes in Kv1.3 mRNA, the inwardly rectifying current decreased in microglia (19). In addition, transforming growth factor-β, a deactivating cytokine, induces Kv1.3 without any relevant effect on the inward current (52). In contrast, THP-1 phorbol 12-myristate 13-acetate-differentiated macrophages decreased Kv1.3 concomitantly to an increase in Kir2.1 (15). Our results suggest that LPS-induced activation regulates VDPC differentially, probably fine tuning the membrane potential and discriminating them from proliferative signals that require more negative values.

By inducing Kv1.3 and repressing Kir2.1, macrophages reduce the Ca^{2+} driving force, the intracellular K^+ concentration ($[K^+]_i$), and the membrane potential hyperpolarization. While an increase in Ca^{2+} initiates the mitogenic pathway, LPS-induced activation does not mobilize Ca^{2+} in macrophages (53). LPS activates macrophages and generates apoptosis in several cell types (25). Kv1.3 functions relatively early in the pro-apoptotic cascade in T-cells and neurons (54, 55). In addition, a decrease in $[K^+]_i$ is involved in the formation of the apoptosome (56). This is consistent with the Kv1.3 and Kir2.1 regulation that we observed. Thus, a loss of cytosolic K^+ is related to thymocyte apoptosis and partially protected by blocking K^+ channels (57). On the other hand, VDPC blockers and depolarizing agents cause $p27^{kip1}$ and $p21^{cip1(waf-1)}$ accumulation and G_1 arrest in oligodendrocyte progenitors (58). Furthermore, a $p21^{cip1(waf-1)}$ increase is associated with the cell growth inhibition in interferon-γ-activated macrophages (59). However, although $p21^{cip1(waf-1)}$ could play a role in the inhibition of macro-

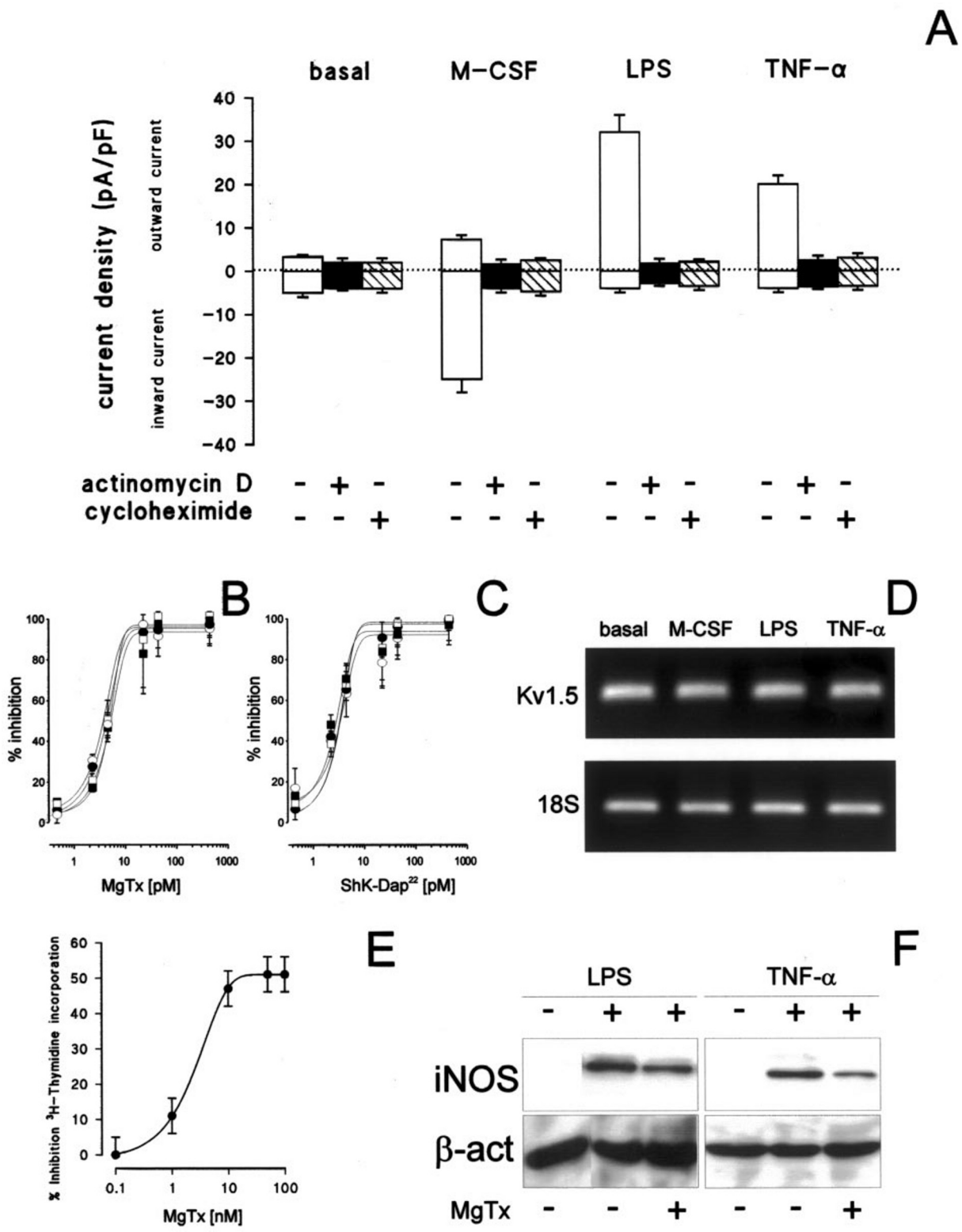

FIG. 9. **VDPC regulation is dependent on *de novo* mRNA and protein synthesis and Kv1.3 is involved in BMDM activation and proliferation.** Macrophages were cultured in the absence of M-CSF for 18 h, then G_0-arrested cells were further incubated for 24 h in the absence (*basal*) or presence of M-CSF with or without LPS or TNF-α. *A*, regulation of K^+ currents is dependent on *de novo* synthesis of mRNA and protein. K^+ current induction was inhibited by the addition of either 5 μg/ml actinomycin D (*closed bars*) or 5 μg/ml cycloheximide (*hatched bars*) during the treatment. Cells were held at −60 mV and currents were elicited by depolarizing pulses of +50 mV (outward current) and hyperpolarizing pulses of −150 mV (inward currents). Values are the mean ± S.E. of at least six independent cells. *B* and *C*, inhibition of the outward K^+ current by MgTx and ShK-Dap^{22}, respectively. ○, basal; ●, M-CSF; □, LPS; ■, TNF-α. *D*, Kv1.5 mRNA expression analyzed by RT-PCR in BMDM. See "Experimental Procedures" for details. *E*, MgTx inhibits M-CSF-dependent proliferation in macrophages. Macrophages were cultured in the absence of M-CSF for 18 h. Cells were further incubated during 24 h with or without the growth factor (1200 units/ml) in the presence of increasing concentrations of MgTx. Sample collection was performed as described under "Experimental Procedures." Values are the mean ± S.E. of four different assays each done in triplicate. *F*, Kv1.3 is involved in the LPS- and TNF-α-induced activation. Proliferating macrophages were cultured during 24 h in the absence (−) or presence (+) of LPS and TNF-α with or without 10 nM MgTx. iNOS protein expression was determined as described under "Experimental Procedures." A representative Western blot of three independent experiments is shown.

phage proliferation by K^+ channels, other mechanisms may be involved. Thus, cyclin D, essential for G_1/S progression, is regulated by extracellular signals (59). In this context, the induction of Kv1.3 associated with a Kir2.1 decrease would increase the extracellular K^+ concentration. Similar depolarization activates T-cell β_1 integrin moieties initiating T-cell immune reactions (60).

Role of TNF-α—Most of the effects of LPS during endotoxic shock are associated with the secretion of TNF-α by tissue macrophages (25). TNF-α affects the growth and function of many cell types, and is a major mediator of inflammatory immune responses upon the activation of p55 type I and p75 type II receptors (61). Several lines of evidence implicate TNF-α in LPS-induced regulation of VDPC. First, TNF-α blocks proliferation and is involved in several LPS-induced mechanisms such as apoptosis and nucleoside transport (25, 35). Second, the time course of VDPC regulation probably coincides with the early induction of TNF-α mRNA expression (25). Finally, the production of TNF-α requires K^+ channel activity (62).

TNF-α mimicked the LPS differential regulation of VDPC. However, this affirmation is only partially correct. Whereas the effects on Kir2.1 were similar, Kv1.3 showed some differences. Results on current densities and knockout mice suggest that LPS regulation involves TNF-α−dependent and -independent mechanisms. Indeed, TNF-α inhibits cell proliferation but the further addition of either MgTx or Ba^{2+} was additive.

In the bone marrow, TNF-α induces DNA fragmentation and cell death by apoptosis (25, 35). The activation of caspase 8 initiates the cascade of caspases that leads to apoptosis, apparently without any second messengers (25). However, alterations in ion composition regulate the activity of effector caspases and nucleases, thereby regulating pro-apoptotic signals (63). As indicated above, differential regulation of VDPC could modify this intracellular ion composition. Indeed, a +25 mV change modifies IL-2 production, thus reducing the activation and the antibody production by lymphocytes (50). Thus, differences between the LPS and TNF-α regulation of Kv1.3 and Kir2.1 currents could separate the two situations triggering the required and specific immune response.

Evidence for Post-translational Control of Kv1.3 during Activation—Ion channels are under extensive regulation, and changes among expression levels have been reported. However, in long term studies, VDPC mRNA mostly governs protein and activity (13, 34, 36). Although our results indicate that VDPC are mainly regulated at the transcriptional level, which is translated to protein abundance, which in turn would be responsible for changes in current amplitudes, other alternative mechanisms, such as changes in mRNA stability, should not be discarded.

While M-CSF-dependent proliferation did not modify the steady-state activation curves for Kv1.3 and Kir2.1, LPS and TNF-α reduced the *k* value of Kv1.3. Previous studies suggest that K^+ channels are involved in T-cell activation and provide evidence of post-translational processes. Thus, Kv1.3 could be phosphorylated by several kinases (38, 47). In addition, conformational changes of the K^+ channel structure are possible by high K^+ concentrations outside the T-cell (60). Finally, the heteromeric structure of the Kv1.3 associated with Kv1.5 and Kvβ regulatory subunits could define a wide diversity of physiological activities and immunological functions (64). Indeed, LPS induces Kvβ1.1 and Kvβ2.1 in T-cells and splenocytes (65). Changes in Kvβ subunits during macrophage activation could indeed modify the kinetics of the *de novo* synthesized K^+ channels as observed during myogenesis (34). Work is in progress in our laboratory to elucidate the role of these modulatory subunits and some preliminary results have been recently described (66).

In summary, we provide strong evidence that proliferation and activation require specific VDPC modulation that would determine appropriate signals for each process. Furthermore, VDPC regulation by LPS implies redundant pathways in which the endotoxin participates by TNF-α-dependent and -independent mechanisms that would trigger differential responses. Our results have physiological significance because the channels might control the cell physiology and their activity may also be modulated by changes in the K^+ gradient. Thus, a loss of $[K^+]_i$ occurs in immunologically relevant situations such as cellular injury, stress, and inflammation (60). In this context, VDPC could buffer K^+ and modulate cellular responses. Finally, our results indicate that K^+ channels should be considered as pharmacological targets in anti-inflammatory and immunomodulation therapies.

Acknowledgments—We thank R. Martínez and S. Ruiz for excellent technical assistance, L. Martín and J. Bertrán for help with macrophage cultures, and Drs. F. J. López-Soriano and J. M. Argilés for kindly providing TNF-α receptor I/II double knockout mice. We are particularly indebted to Prof. M. M. Tamkun (Colorado State University) for critically reading the manuscript. The editorial assistance of Robin Rycroft (University of Barcelona linguistic bureau, SAL) and Tanya Yates is also acknowledged.

REFERENCES

1. Ogawa, M. (1993) *Blood* **81,** 2844–2853
2. Celada, A., and Nathan, C. (1993) *Immunol. Today* **15,** 100–102
3. Hille, B. (2001) *Ion Channels of Excitable Membranes*, 3rd Ed., Sinauer Associates, Sunderland, MA
4. Gallin, E. K., and Livengood, D. R. (1981) *Am. J. Physiol.* **241,** C9–C17
5. Gallin, E. K. (1984) *Biophys. J.* **46,** 821–825
6. Ypey, D. L., and Clapham, D. E. (1984) *Proc. Natl. Acad. U. S. A.* **81,** 3083–3087
7. Gallin, E. K., and Sheehy, P. A. (1985) *J. Physiol.* **369,** 475–499
8. Gallin, E. K., and McKinney, L. C. (1988) *J. Membr. Biol.* **103,** 55–66
9. McKinney, L. C., and Gallin, E. K. (1988) *J. Membr. Biol.* **103,** 41–53
10. Gallin, E. K. (1989) *Am. J. Physiol.* **257,** C77–C85
11. McKinney, L. C., and Gallin, E. K. (1992) *J. Membr. Biol.* **130,** 265–276
12. Judge, S. I., Montcalm-Mazzilli, E., and Gallin, E. K. (1994) *Am. J. Physiol.* **267,** C1691–C1698
13. DeCorsey, T. E., Kim, S. Y., Silver, M. R., and Quandt, F. N. (1996) *J. Membr. Biol.* **152,** 141–157
14. Eder, C., Klee, R., and Heinemann, U. (1997) *Naumyn-Schmiedeberg's Arch. Pharmacol.* **356,** 233–239
15. Schmid-Antomarchi, H., Schmid-Alliana, A., Romey, G., Ventura, M. A., Breittmayer, V., Millet, M. A., Husson, H., Moghrabi, B., Lazdunski, M., and Rossi, B. (1997) *J. Immunol.* **159,** 6209–6215
16. Colden-Stanfield, M., and Gallin, E. K. (1998) *Am. J. Physiol.* **275,** C267–C277
17. Qiu, M. R., Campbell, T. J., and Breit, S. N. (2002) *Clin. Exp. Immunol.* **130,** 67–74
18. Gallin, E. K. (1991) *Physiol. Rev.* **71,** 775–811
19. Eder, C. (1998) *Am. J. Physiol.* **275,** C327–C342
20. DeCoursey, T. E., and Grinstein, S. (1999) in *Inflammation: Basic Principles and Clinical Correlates* (Gallin, J. I., and Snyderman, R., eds) pp. 141–157, Lippincott Willians & Wilkins, Philadelphia, PA
21. Blunck, R., Scheel, O., Müller, M., Brandenburg, K., Seitzer, U., and Seydel, U. (2001) *J. Immunol.* **166,** 1009–1015
22. Soler, C., García-Manteiga, J., Valdés, R., Xaus, J., Comalada, M., Casado, F. J., Pastor-Anglada, M., Celada, A., and Felipe, A. (2001) *FASEB J.* **15,** 1979–1988
23. Stanley, E. R., Berg, K. L., Einstein, D. B., Lee, P. S., Pixley, F. J., Wang, Y., and Yeung, Y. G. (1997) *Mol. Reprod. Dev.* **46,** 4–10
24. Sweet, M. J., and Hume, D. A. (1996) *J. Leukocyte Biol.* **60,** 8–26
25. Xaus, J., Comalada, M., Valledor, A. F., Lloberas, J., López-Soriano, F. J., Argilés, J. M., Bogdan, C., and Celada, A. (2000) *Blood* **95,** 3823–3831
26. Garcia-Calvo, M., Leonard, R. J., Novick, J. N., Stevens, S. P., Schmalhofer, W., Kaczorowski, G. J., and Garcia, M. L. (1993) *J. Biol. Chem.* **268,** 18866–18874
27. Kalman, K., Pennington, M. W., Lanigan, M. D., Nguyen, A., Rauer, H., Mahnir, V., Paschetto, K., Kem, W. R., Grissmer, S., Gutman, G. A., Christian, E. P., Cahalan, M. D., Norton, R. S., and Chandy, K. G. (1998) *J. Biol. Chem.* **273,** 32697–32707
28. Lepple-Wienhues, A., Berweck, S., Böhmig, M., Leo, C. P., Meyling, B., Garbe, C., and Wiederholt, M. (1996) *J. Membr. Biol.* **151,** 149–157
29. Celada, A., Klemsz, M. J., and Maki, R. A. (1989) *Eur. J. Immunol.* **19,** 1103–1109
30. Cullel-Young, M., Barrachina, M., López-López, C., Goñalons, E., Lloberas, J., Soler, C., and Celada, A. (2001) *Immunogenetics* **53,** 136–144
31. Bruce, A. J., Boling, W., Kindy, M. S., Peschon, J., Kraemer, P. J., Carpenter, M. K., Holtsberg, F. W., and Mattson, M. P. (1996) *Nat. Med.* **2,** 788–794
32. Fuster, G., Vicente, R., Coma, M., Grande, M., and Felipe, A. (2002) *Methods Find. Exp. Clin. Pharmacol.* **24,** 253–259

33. Coma, M., Vicente, R., Busquets, S., Carbó, N., Tamkun, M. M., López-Soriano, F. J., Argilés, J. M., and Felipe, A. (2003) *FEBS Lett.* **536,** 45–50
34. Grande, M., Suàrez, E., Vicente, R., Cantó, C., Coma, M., Tamkun, M. M., Zorzano, A., Gumà, A., and Felipe, A. (2003) *J. Cell. Physiol.* **195,** 187–193
35. Soler, C., Valdés, R., García-Manteiga, J., Xaus, J., Comalada, M., Casado, F. J., Modolell, M., Nicholson, B., MacLeod, C., Felipe, A., Celada, A., and Pastor-Anglada, M. (2001) *J. Biol. Chem.* **276,** 30043–30049
36. Chittajallu, R., Chen, Y., Wang, H., Yuan, X., Ghiani, C. A., Heckman, T., McBain C. J., and Gallo, V. (2002) *Proc. Natl. Acad. Sci. U. S. A.* **99,** 2350–2355
37. Lowry, M. A., Goldberg, J. I., and Belosevic, M. (1998) *Clin. Exp. Immunol.* **111,** 597–603
38. Cahalan, M. D., Wulff, H., and Chandy, K. G. (2001) *J. Clin. Immunol.* **21,** 235–252
39. Wieland, S., Chou, R. H., and Gong, Q. H. (1990) *J. Cell. Physiol.* **142,** 643–651
40. Nelson, D. J., Jow, B., and Jow, F. (1992) *J. Membr. Biol.* **125,** 201–218
41. Lu, L., Yang, T., Markakis, D., Guggino, W. B., and Craig, R. W. (1993) *J. Membr. Biol.* **132,** 267–274
42. Eder, C., and Fischer, H. G. (1997) *Arch. Pharmacol.* **355,** 198–202
43. Attali, B., Romey, G., Honoré, E., Scmid-Alliana, A., Mattéi, M. G., Lesage, F., Ricard, P., Barhanin, J., and Lazdunski, M. (1992) *J. Biol. Chem.* **267,** 8650–8657
44. Freedman, B. D., Fleischmann, B. K., Punt, J. A., Gaulton, G., Hashimoto, Y., and Kotlikoff, M. I. (1995) *J. Biol. Chem.* **270,** 22406–22411
45. Kotecha, S. A., and Schlicheter, L. C. (1999) *J. Neurosci.* **19,** 10680–10693
46. Sobko, A., Perezt, A., Shirihai, O., Etkin, S., Cherepanova, V., Dagan, D., and Attali, B. (1998) *J. Neurosci.* **18,** 10398–10408
47. Holmes, T. C., Fadool, D. A., and Levitan, I. B. (1996) *J. Neurosci.* **16,** 1581–1590
48. Holmes, T. C., Berman, K., Swartz, J. E., Dagan, D., and Levitan, I. B. (1997) *J. Neurosci.* **17,** 8964–8974
49. Fischer-Lougheed, J., Liu, J. H., Espinos, E., Mordasini, D., Bader, C. R., Belin, D., and Bernheim, L. (2001) *J. Cell Biol.* **153,** 677–685
50. Freedman, B. D., Price, M. A., and Deutsch, C. J. (1992) *J. Immunol.* **149,** 3784–3794
51. Berridge, M. J. (1993) *Nature* **361,** 315–325
52. Schilling, T., Quandt, F. N., Cherny, V. V., Zhou, W., Heinemann, U., DeCoursey, T. E., and Eder, C. (2000) *Am. J. Physiol.* **279,** C1123–C1134
53. Valledor, A. F., Xaus, J., Comalada, M., Soler, C., and Celada, A. (2000) *J. Immunol.* **164,** 29–37
54. Bock, J., Szabó, I., Jekle, A., and Gulbins, E. (2002) *Biochem. Biophys. Res. Commun.* **295,** 526–531
55. Yu, S. P., Yeh, C. H., Gottron, F., Wang, X., Grabb, M. C., and Choi, D. W. (1999) *J. Neurochem.* **73,** 933–941
56. Cain, K., Langlais, C., Sun, X. M., Brown, D. G., and Cohen, G. M. (2001) *J. Biol. Chem.* **276,** 41985–41990
57. Dallaporta, B., Marchetti, P., de Pablo, M. A., Maisse, C., Duc, H. T., Métivier, D., Zamzami, N., Geuskens, M., and Kroemer, G. (1999) *J. Immunol.* **162,** 6534–6542
58. Ghiani, C. A., Yuan, X., Eisen, A. M., Knutson, P. L., DePinho, R. A., McBain, C. J., and Gallo, V. (1999) *J. Neurosci.* **19,** 5380–5392
59. Xaus, J., Cardó, M., Valledor, A. F., Soler, C., Lloberas, J., and Celada, A. (1999) *Immunity* **11,** 103–113
60. Levite, M., Cahalon, L., Peretz, A., Hershkoviz, R., Sobko, A., Ariel, A., Desai, R., Attali, B., and Lider, O. (2000) *J. Exp. Med.* **191,** 1167–1176
61. Tartaglia, L. A., and Goeddel, D. V. (1992) *Immunol. Today* **13,** 151–153
62. Maruyama, N., Kakuta, Y., Yamauchi, K., Ohkawara, Y., Aizawa, T., Ohrui, T., Nara, M., Oshiro, I., and Tamura, G. (1994) *Am. J. Respir. Cell Mol. Biol.* **10,** 514–520
63. Bortner, C. D., and Cidlowski, J. A. (1999) *J. Biol. Chem.* **274,** 21953–21962
64. McCormack, T., McCormack, K., Nadal, M. S., Vieira, E., Ozaita, A., and Rudy, B. (1999) *J. Biol. Chem.* **274,** 20123–20126
65. Autieri, M. V., Belkowski, S. M., Constantinescu, C. S., Cohen, J. A., and Prystowsky, M. B. (1997) *J. Neuroimmunol.* **77,** 8–16
66. Vicente, R., Escalada, A., Coma, M., Grande, M., Fuster, G., López-Iglesias, C., Solsona, C., and Felipe, A. (2003) *J. Physiol.* **548P,** O20